Islets 2:5, 308-317; September/October 2010; © 2010 Landes Bioscience

Pim3 negatively regulates glucose-stimulated insulin secretion

Gregory Vlacich,[1] Martijn C. Nawijn,[2] Gene C. Webb[1] and Donald F. Steiner[3,*]

[1]Department of Medicine; and [3]Department of Biochemistry and Molecular Biology; University of Chicago; Chicago, IL USA; [2]Division of Molecular Genetics; Netherlands Cancer Institute; Plesmanlaan, Amsterdam; and Laboratory of Allergology and Pulmonary Medicine; Department of Pathology and Medical Biology; University Medical Center Groningen; Groningen, The Netherlands

Key words: insulin secretion, β-cell, signal transduction, Pim3, ERK, SOCS6

Abbreviations: ERK1/2, extracellular signal-regulated kinases 1 and 2; SOCS6, suppressor of cytokine signaling 6; MIN6, murine insulinoma 6

Pancreatic β-cell response to glucose stimulation is governed by tightly regulated signaling pathways which have not been fully characterized. A screen for novel signaling intermediates identified *Pim3* as a glucose-responsive gene in the β-cell, and here, we characterize its role in the regulation of β-cell function. Pim3 expression in the β-cell was first observed through microarray analysis on glucose-stimulated murine insulinoma (MIN6) cells where expression was strongly and transiently induced. In the pancreas, *Pim3* expression exhibited similar dynamics and was restricted to the β-cell. Perturbation of Pim3 function resulted in enhanced glucose-stimulated insulin secretion, both in MIN6 cells and in isolated islets from *Pim3*$^{-/-}$ mice, where the augmentation was specifically seen in the second phase of secretion. Consequently, *Pim3*$^{-/-}$ mice displayed an increased glucose tolerance in vivo. Interestingly, *Pim3*$^{-/-}$ mice also exhibited increased insulin sensitivity. Glucose stimulation of isolated *Pim3*$^{-/-}$ islets resulted in increased phosphorylation of ERK1/2, a kinase involved in regulating β-cell response to glucose. Pim3 was also found to physically interact with SOCS6 and SOCS6 levels were strongly reduced in *Pim3*$^{-/-}$ islets. Overexpression of SOCS6 inhibited glucose-induced ERK1/2 activation, strongly suggesting that Pim3 regulates ERK1/2 activity through SOCS6. These data reveal that Pim3 is a novel glucose-responsive gene in the β-cell that negatively regulates insulin secretion by inhibiting the activation of ERK1/2, and through its effect on insulin sensitivity, has potentially a more global function in glucose homeostasis.

Introduction

Pancreatic β-cells play a vital role in glucose homeostasis by secreting insulin in response to circulating glucose and other nutrient stimuli.[1,2] Glucose metabolism promotes insulin secretion by increasing the ATP-to-ADP ratio within the β-cell resulting in membrane depolarization via closure of ATP-dependent K^+ channels (K_{ATP}-channel) which then stimulates Ca^{2+} influx via L-type Ca^{2+} channels.[2-4] During the second phase of insulin secretion, several K_{ATP}-independent mechanisms, such as GLP1-augmented secretion and the autocrine action of insulin, modulate the amount of insulin secretion.[5,6]

While its role is less established, activation of the p44/p42 mitogen-activated protein (MAP) kinase (also known as ERK1/2) has also been shown to regulate glucose-stimulated insulin secretion.[7] In the β-cell, ERK1/2 can be activated by glucose at physiologically-relevant concentrations (2–20 mM) and by insulin via activation of insulin receptors on the β-cell membrane.[8-11] ERK1/2 has been implicated in regulating glucose-stimulated insulin gene transcription.[8,12] Whereas initial studies suggested that ERK1/2 had no significant impact on secretion,[10,13] more recently, ERK1/2 activation was shown to enhance insulin secretion up to 20 minutes after glucose stimulation, but not over longer periods of time.[7]

With the emerging importance of these secondary signaling pathways in glucose-stimulated insulin secretion, we attempted to identify novel factors involved in regulating the β-cell response to glucose. Using microarray analysis of MIN6 murine insulinoma cells, we revealed that transcription of the serine/threonine kinase Pim3 was strongly upregulated after glucose stimulation. The expression of Pim kinases in the pancreatic β-cell has not been described before. Pim3 is a member of a conserved family of kinases originally identified as proto-oncogenes, and expression of these kinases is stimulated by numerous growth factors and cytokines.[14-16] The Pim kinases are widely expressed and *Pim3* mRNA expression has been observed in tissues such as kidney, pituitary, heart and skeletal muscle.[17-19] Pim3 expression has also been observed in neuronal and neuroendocrine cells where expression is rapidly induced by membrane depolarization.[17] Though their role in untransformed cells is not fully understood, Pim

Correspondence to: Donald F. Steiner; Email: dfsteine@midway.uchicago.edu
Submitted: 06/01/10; Revised: 07/14/10; Accepted: 07/16/10
Previously published online: www.landesbioscience.com/journals/islets/article/13058
DOI: 10.4161/isl.2.5.13058

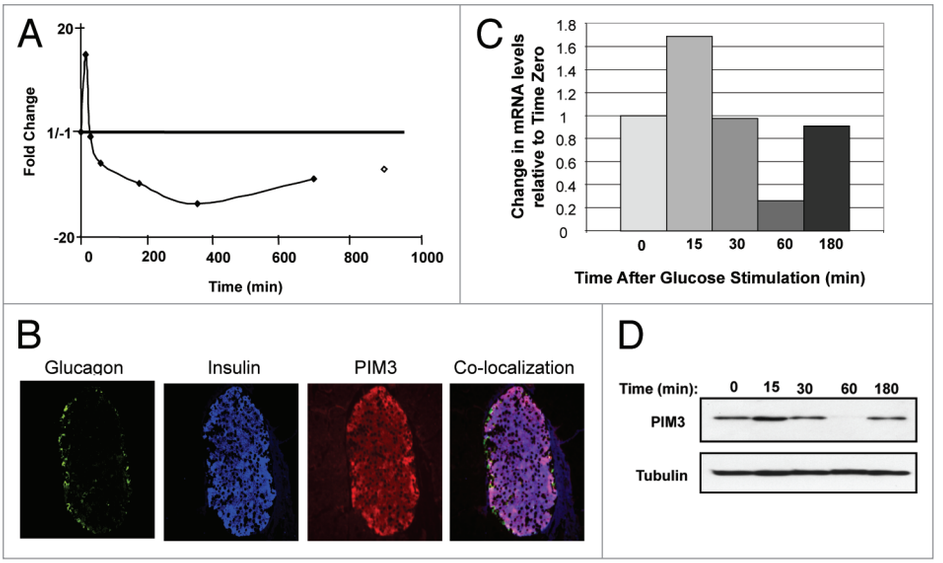

Figure 1. *Pim3* is a glucose-responsive gene expressed exclusively in pancreatic β-cells. (A) Microarray analysis of glucose-stimulated MIN6 cells shows relative (to T_0) *Pim3* transcript abundance at various timepoints after glucose stimulation. Results shown are an average of 2 independent experiments. The open diamond represents *Pim3* mRNA levels under normal growth (25 mM) conditions. (B) Immunofluorescence of representative islets in wildtype mice show that Pim3 (red) co-localizes almost entirely with insulin-positive β-cells (blue, magenta in co-localization panel) and not with glucagon-positive α-cells (green, yellow in co-localization panel) or the surrounding acinar tissue. (C and D) Real time-PCR (C) and immunoblots (D) of wildtype islets show that *Pim3* mRNA and protein are expressed in primary β cells and exhibit an identical expression profile after glucose stimulation that is similar to that seen in MIN6 cells. Results shown are representative of 2 (C) or 3 (D) independent experiments.

kinases have been shown to phosphorylate and stabilize suppressor of cytokine signaling (SOCS) family members, thereby regulating signal transduction via Jak/STAT and other pathways.[20,21] In addition, Pim kinases have been shown to phosphorylate Ser^{112} on the pro-apoptotic protein BAD, causing binding to 14-3-3 and dissociation from Bcl-X_L thereby promoting cell survival.[22,23]

To determine if the expression of Pim3 in β-cells regulates β-cell function, we assessed the impact of Pim3 activity in MIN6 cells and primary pancreatic islets. We show that Pim3 negatively regulates the second phase of glucose-stimulated insulin secretion, both in vitro and in vivo. Furthermore, we show that Pim3 expression in pancreatic β-cells results in stabilization of SOCS6, a known negative regulator of the ERK1/2 signaling pathway. The identification of Pim3 and the elucidation of its role in the β-cell thus uncover a novel component in the regulation of insulin secretion with the potential for a broader role in regulating β-cell activity in response to glucose stimulation.

Results

Identification of Pim3 as a glucose-responsive gene in pancreatic β-cells. To identify novel signaling components in the β-cell, we performed microarray analysis on glucose-stimulated murine insulinoma 6 (MIN6) cells. The accuracy and reproducibility of genechip microarray for identifying glucose-responsive β-cell genes in MIN6 cells was previously confirmed.[24] In our study, we identified *Pim3* as a novel gene that exhibited profound changes in expression after glucose stimulation. At 15 minutes after stimulation with 25 mM glucose, there was an average 18-fold increase in *Pim3* mRNA levels. Subsequently, there was a sharp drop in transcript levels at 30 minutes with a further reduction below baseline, followed by a slow recovery in expression (**Fig. 1A**). Though expressed elsewhere, the presence of Pim3 in the pancreatic β-cell has not been previously documented or explored.[17-19]

To confirm the presence of Pim3 in primary islet β-cells, we then examined Pim3 expression via immunofluorescence. In mouse islets, Pim3 is readily detected in the insulin-positive β-cells, but is absent from glucagon-positive α cells and surrounding acinar tissue (**Fig. 1B**).

Next, we examined the dynamics of glucose-stimulated *Pim3* expression in isolated islets. *Pim3* mRNA levels increase sharply 15 minutes after glucose stimulation of islet β-cells, with a subsequent decline in expression until 60 minutes after stimulation, mirroring the observations in MIN6 cells. By 3 hours, the amount of *Pim3* mRNA approaches baseline levels (**Fig. 1C**). The reduced fold-change in *Pim3* transcription compared to MIN6 cells may reflect altered dynamics of glucose stimulation from slower glucose permeation into islets (versus a MIN6 monolayer) and an experimental protocol which utilizes a shorter, more physiologic quiescence of the islets in low glucose. Pim3 protein levels after glucose stimulation closely follow the kinetics of the *Pim3* transcript in the islets (**Fig. 1D**), indicating that *Pim3* expression after stimulation is largely regulated at the level of transcription. This is consistent with the known regulation of Pim1 and Pim2 observed in other cell types.[25,26] Furthermore, the dynamics of Pim3 expression observed here underscore the previously reported instability of Pim family transcripts and proteins. Pim3 mRNA shares a destabilization motif in the 3' untranslated region with Pim1 and Pim2 mRNA and Pim family proteins were found to have a remarkably short half-life (10 minutes or 1 hour).[19,27,28]

Pim3 modulates insulin secretion in MIN6 cells. To determine whether Pim3 expression after glucose stimulation impacts β-cell function, we expressed kinase-dead (KD) Pim3 ($Pim3^{K68R}$) in MIN6 cells and evaluated changes in insulin synthesis or secretion. $Pim3^{K68R}$ carries a point mutation in the ATP-binding pocket rendering it inactive (data not shown). Neither insulin gene transcription nor proinsulin synthesis after glucose stimulation were significantly altered in the presence of KD-Pim3 (data not shown). On the other hand, MIN6 expressing KD-Pim3 show augmented insulin secretion by 60 minutes after glucose stimulation when compared to control-infected MIN6 (**Fig. 2A**),

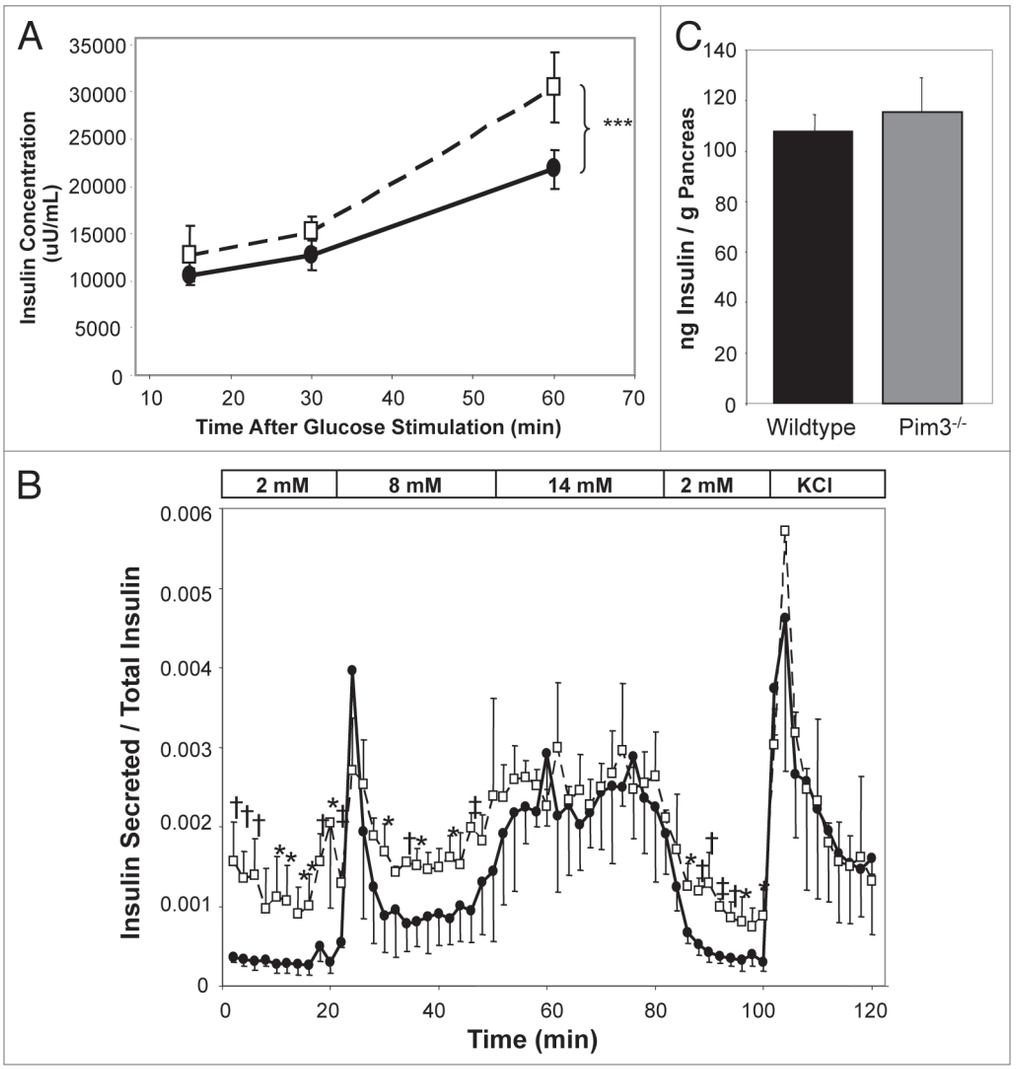

Figure 2. Disruption of Pim3 function leads to an augmentation in glucose-stimulated insulin secretion but has no effect on total insulin levels. (A) MIN6 cells were infected with adenovirus expressing KD-Pim3 (dashed line, open square) or β-gal (solid black line, filled circle), then stimulated with 25 mM glucose and insulin levels were determined 15, 30 and 60 minutes after stimulation. n = 4 each. ***p = 0.006. (B) *Pim3*$^{-/-}$ (dashed line, open square) and wildtype (solid black line, filled circle) islets were isolated and glucose-stimulated insulin secretion was determined by perifusion. Islets (45–50 per sample) were stimulated with 8 mM then 14 mM glucose from 2 mM glucose KRB and finally with 30 mM KCl in 2 mM glucose. Fractions were collected every 2 minutes at a flow rate of 0.5 mL/min. Data are represented as insulin secreted in each fraction divided by total insulin content of the islets in each perifusion chamber. n = 3 for each genotype. *p < 0.05, †p ≤ 0.01, ‡p < 0.001. (C) Total insulin levels of *Pim3*$^{-/-}$ (gray bar) and wildtype (black bar) were determined by acid-ethanol extraction. n = 5, wt; n = 4, *Pim3*$^{-/-}$.

suggesting Pim3 may negatively regulate glucose-stimulated insulin secretion.

***Pim3*$^{-/-}$ islets exhibit enhanced glucose-stimulated insulin secretion with total insulin levels unaffected.** To validate the observed effects of Pim3 on insulin secretion, we analyzed islets from *Pim3*$^{-/-}$ mice generated by Mikkers et al. which were reported to lack any overt phenotype.[19] We evaluated glucose-stimulated insulin secretion by stimulation with 8 mM (suboptimal) and 14 mM (optimal) glucose in perifusion studies. Strikingly, *Pim3*$^{-/-}$ islets had a significantly increased basal rate of insulin secretion at 2 mM glucose (**Fig. 2B**). After stimulation with 8 mM glucose, wild-type islets responded normally with a sharp peak in insulin secretion (first phase) followed by an elevated-but-flat second phase (**Fig. 2B**). In contrast, *Pim3*$^{-/-}$ islets displayed a blunted first phase, followed by a second phase which was elevated as compared to wildtype. Remarkably, the responses of wildtype and *Pim3*$^{-/-}$ islets to 14 mM glucose are almost identical. Also, insulin release induced by KCl treatment (in 2 mM glucose) was comparable between the two genotypes (**Fig. 2B**). Total pancreatic insulin content did not differ significantly between *Pim3*$^{-/-}$ and wildtype islets (**Fig. 2C**), implying that the enhanced insulin secretion in *Pim3*$^{-/-}$ islets was not due to the presence of enlarged intracellular stores.

***Pim3*$^{-/-}$ mice show increased insulin sensitivity and improved glucose tolerance.** To further examine how Pim3 impacts glucose homeostasis in vivo, we evaluated *Pim3*$^{-/-}$ mice

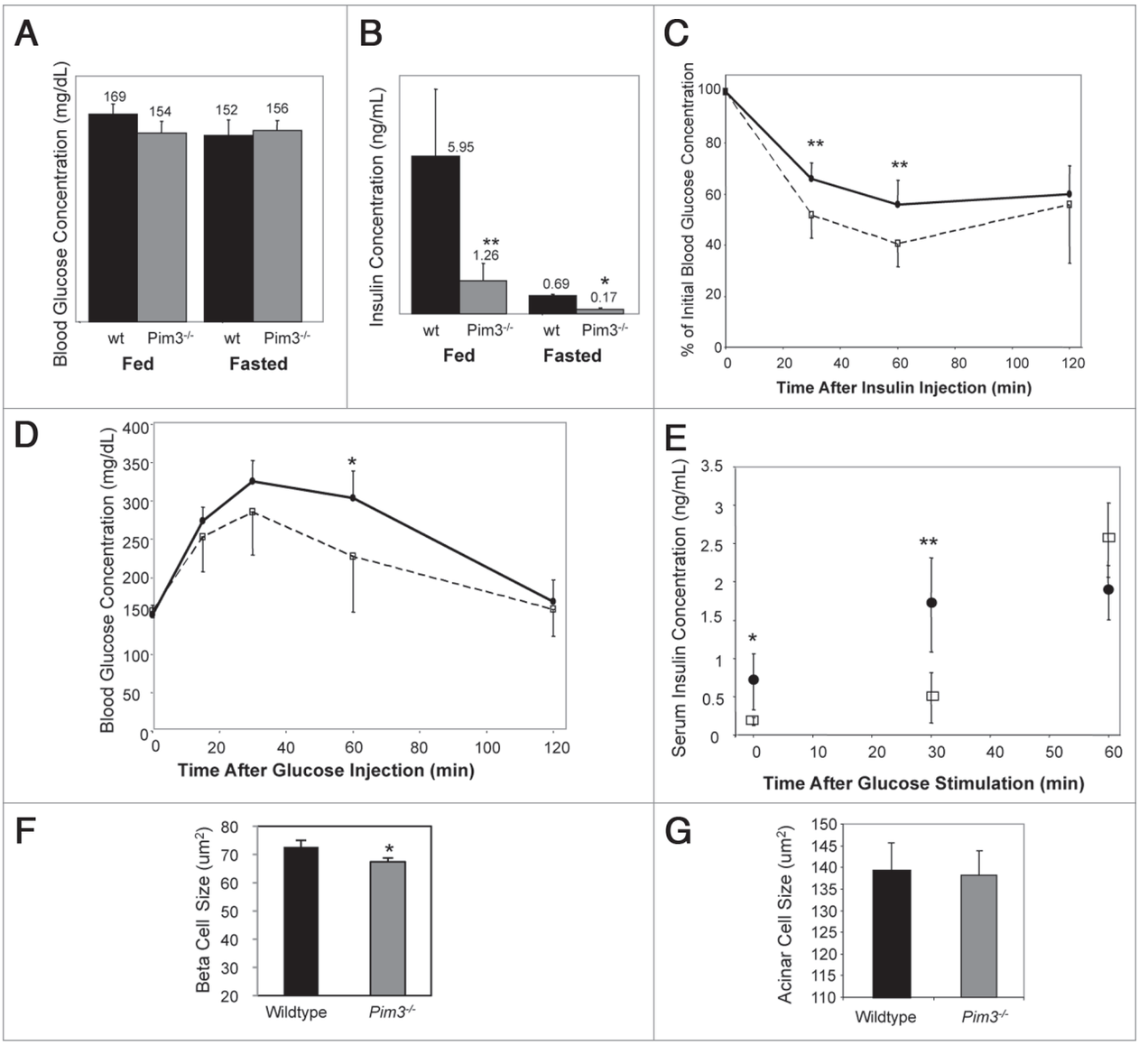

Figure 3. *Pim3*$^{-/-}$ mice exhibit increased insulin sensitivity and improved glucose tolerance. Blood glucose (A) and serum insulin levels (B) were determined in freely fed and fasted (overnight) *Pim3*$^{-/-}$ (grey bar) and wildtype (black bar) mice. For fed serum insulin: n = 5, wt; n = 4, *Pim3*$^{-/-}$. For fasted serum insulin: n = 4, wt; n = 3, *Pim3*$^{-/-}$. Blood glucose levels were also evaluated during an insulin (C) and glucose (D) tolerance test with wildtype (solid black line, filled circle) and *Pim3*$^{-/-}$ (dashed line, open square) mice. Mice were all male between 10 and 16 weeks of age. For blood glucose levels and insulin and glucose tolerance tests: n = 9, wt; n = 5, *Pim3*$^{-/-}$. (E) Serum insulin levels were monitored in wildtype (filled circle) and *Pim3*$^{-/-}$ (open square) mice during a glucose tolerance test. n = 3, wt and *Pim3*$^{-/-}$. *p < 0.05, **p ≤ 0.025. (F and G) Average beta cell size (F) was calculated for each islet examined and wildtype (black bar) and *Pim3*$^{-/-}$ (grey bar) averages compared. Beta cells from *Pim3*$^{-/-}$ mice are, on average, approximately 6.5% smaller than wildtype beta cells. Average acinar cells size (G) was determined from acinar cells surrounding islets. Beta cells: n = 68 islets, wildtype; n = 64 islets, *Pim3*$^{-/-}$. Acinar cells: n = 72 regions, wildtype and *Pim3*$^{-/-}$. *p = 0.0069.

for putative alterations in glucose or insulin levels. Under steady-state conditions, blood glucose concentrations did not vary much (**Fig. 3A**). However, serum insulin levels were significantly reduced in Pim3$^{-/-}$ mice compared to wildtype (**Fig. 3B**), an especially surprising result considering the elevated basal secretion seen in the perifusion study. This suggests the Pim3$^{-/-}$ mice have enhanced peripheral insulin sensitivity. Indeed, increased insulin sensitivity was observed in *Pim3*$^{-/-}$ mice at 30 and 60 minutes after insulin stimulation (**Fig. 3C**). Additionally, average β-cell size is slightly, but significantly and specifically reduced in *Pim3*$^{-/-}$ mice (**Fig. 3F and G**), consistent with a decreased in vivo demand for insulin.

At the β-cell level, our in vitro data point towards increased glucose-stimulated insulin secretion in the absence of Pim3 and this was confirmed in vivo. A glucose tolerance test demonstrates that *Pim3*$^{-/-}$ mice display enhanced glucose uptake relative to wildtype (**Fig. 3D**). At earlier time points, the trend towards improved glucose tolerance is likely the result of enhanced insulin sensitivity as serum insulin level are reduced in *Pim3*$^{-/-}$ mice (**Fig. 3E**). However, serum insulin levels at 60 minutes suggest that

this improved mobilization of glucose is a result of late enhancement of insulin secretion between 30 and 60 minutes after glucose stimulation (**Fig. 3E**) coincident with the accelerated glucose uptake in *Pim3*$^{-/-}$ mice at 60 minutes (**Fig. 3D**).

Pim3 inhibits ERK1/2 activation with minimal effect on Akt. The specific effects of Pim3 on the second phase of insulin secretion as well as documented roles for the other Pim family proteins in the regulation of signal transduction[25,29] suggest that Pim3 may be affecting insulin secretion by functioning in one or more glucose-stimulated or glucose-requiring K_{ATP}-independent regulatory pathways.[5-7] Potential pathways include those that function through the activation of Akt and ERK1/2.[7,11,30] To determine whether Pim3 functions through either of these kinases, isolated islets from *Pim3*$^{-/-}$ and wildtype mice were stimulated with glucose and analyzed for activation of ERK1/2 and Akt. Indeed, *Pim3*$^{-/-}$ islets have more activated ERK1/2 both at 5 and 10 minutes after stimulation with no difference in the levels of phosphorylated Akt (**Fig. 4**). This suggests that Pim3 functions as a negative regulator of the ERK1/2 pathway with no effect on Akt. Preliminary perifusion studies in the presence of the MEK inhibitor PD98059 further suggest that Pim3 regulates insulin secretion through this effect on ERK1/2 activation as the increased secretion seen in untreated *Pim3*$^{-/-}$ islets (**Fig. 2B**) is abolished when ERK1/2 phosphorylation is inhibited (**Suppl. Fig. 1**).

Pim3 acts on the ERK1/2 pathway through interaction with SOCS6. Pim kinases have previously been shown to phosphorylate and stabilize members of the suppressor of cytokine signaling (SOCS) family, thus enhancing their ability to negatively regulate signaling pathways.[20,21] To evaluate whether Pim3 may regulate ERK1/2 activity in β-cells through an effect on SOCS, we performed GST pull-down assays using wildtype (wt) and KD-Pim3-GST fusion proteins with MIN6 cell lysate. All SOCS family members except SOCS2 are expressed in MIN6 cells (data not shown), though Pim3-GST appeared to associate only with SOCS3, SOCS5 and SOCS6 (**Fig. 5A**). In contrast, Pim3-GST did not directly associate with components of the ERK1/2 pathway (data not shown). We then confirmed the observed interactions with SOCS proteins through crosslinking analysis in MIN6 cells expressing an HA-tagged form of KD-Pim3 (wildtype Pim3 was toxic to the bacterial host used to construct the recombinant adenovirus and so could not be used in these experiments). Under these conditions, only SOCS6 was found to interact with Pim3 (**Fig. 5B**). The relative levels of SOCS6 correlated well with the relative level of Pim3 expressed from the transfected vector and immunoprecipitated, further supporting a direct and specific interaction (**Fig. 5B**).

In parallel to the observed effects of Pim kinases on SOCS protein levels, we hypothesized that SOCS6 stability would be enhanced through Pim3 phosphorylation.[20,21] To test this, we compared SOCS6 levels in *Pim3*$^{-/-}$ versus wildtype islets. In the absence of Pim3, there is a substantial reduction in the amount of SOCS6 present under normal growth conditions (**Fig. 5C**), suggesting Pim3 regulates SOCS6 stability in the β-cell. It is likely that the increased stability of SOCS6 in the presence of Pim3 is the result of SOCS6 phosphorylation, as we can demonstrate

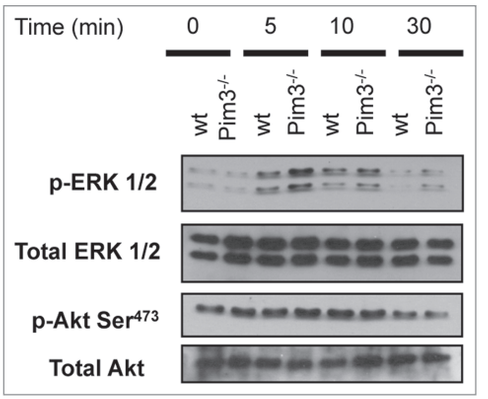

Figure 4. Pim3 negatively regulates the ERK1/2 signaling pathway. Isolated islets (40–45 per timepoint) from *Pim3*$^{-/-}$ and wildtype mice were treated with 2.8 mM glucose RPMI for 3 hours and stimulated with 16.7 mM glucose RPMI for the times indicated and levels of activated signal components determined through immunoblot. Results shown are representative of 3 independent experiments.

that SOCS6 and Pim3 physically interact (**Fig. 5A and B**) and Pim3 phosphorylation of other SOCS proteins is known to lead to increased stability.[20,21]

Numerous studies have implicated SOCS6 in the negative regulation of ERK1/2 activity in other cell types in response to various stimuli.[31-33] To determine whether SOCS6 can regulate glucose-mediated ERK1/2 activation in the β-cell, we examined glucose-stimulated signaling in MIN6 cells stably overexpressing SOCS6. Consistent with its role as a negative regulator, activation of ERK1/2 was significantly reduced with SOCS6 overexpression (**Fig. 5D**). This reduced phosphorylation of ERK1/2 with SOCS6-overexpression compared with the increased ERK1/2 phosphorylation in *Pim3*$^{-/-}$ islets (which exhibit strongly reduced SOCS6 levels) suggest that Pim3 can modify activity of the ERK1/2 pathway through SOCS6. Furthermore, SOCS6 seems to preferentially affect ERK1/2 activity since MEK phosphorylation is not significantly affected (**Fig. 5D**).

Discussion

Glucose stimulation of the pancreatic β-cell triggers a number of downstream events that result in insulin secretion.[1,2] In an effort to uncover novel participants in these signaling pathways, we identified the serine/threonine kinase *Pim3* as a novel glucose-responsive gene in the β-cell. Although Pim3 is expressed in a number of tissues including other neuroendocrine cells, neither the presence nor the function of Pim3 has been characterized in β-cells.[17-19] We show that Pim3 expression within the pancreas is confined to the β-cells, where Pim3 acts as a negative regulator of the second phase of glucose-stimulated insulin secretion.

Enhanced insulin secretion in response to glucose stimulation is seen in both MIN6 cells overexpressing KD-Pim3 and islets isolated from *Pim3*$^{-/-}$ mice. Perifusion studies on isolated islets revealed that this augmentation in insulin secretion occurs primarily with low (8 mM) glucose stimulation, and during the

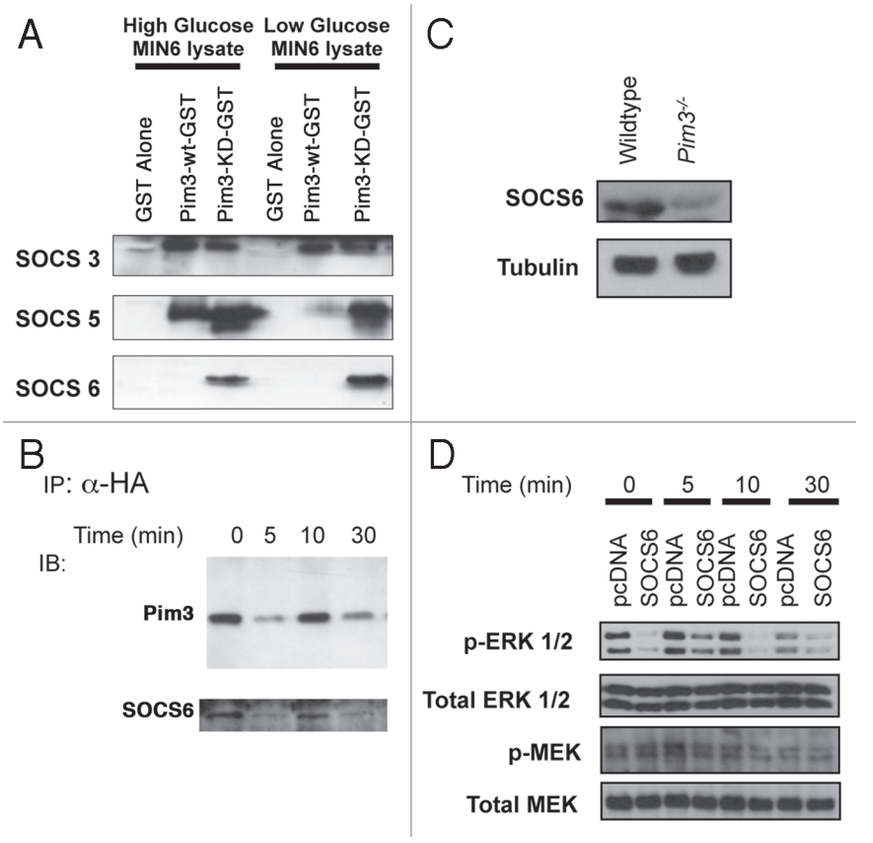

Figure 5. Pim3 directly interacts with SOCS6 and this interaction may mediate its effect on ERK1/2. (A) GST pulldown experiment using MIN6 cell lysates from cells grown in either high (25 mM) or low (0.5 mM) glucose conditions and wt-Pim3-GST, KD-Pim3-GST fusion proteins or GST alone as bait. Possible interactions were evaluated by western blot. (B) Crosslinking experiments using MIN6 infected with adenovirus expressing HA-tagged form of KD-Pim3. MIN6 cells were infected with KD-HA-Pim3 adenovirus, incubated in 0.5 mM glucose for 3 hours then stimulated with 25 mM glucose for the times indicated. Cells were lysed in 1% Triton X-100 buffer containing 1.25 mM DTSSP, Pim3 was immunoprecipitated with α-HA antibody, and associated proteins identified by western blot. (C) Islets under normal growth (11.5 mM glucose) conditions were lysed and levels of SOCS6 and tubulin determined by western blot. (D) MIN6 cells stably overexpressing SOCS6 were incubated in 0.5 mM glucose for 3 hours and then stimulated with 25 mM glucose for the times indicated. Cells were lysed and protein levels determined by western blot.

second phase. Heterogeneity in the glucose responsiveness of β-cell populations may account for this unique phenotype of *Pim3*$^{-/-}$ islets. Stimulation with 7.5 mM glucose activates approximately 50% of isolated β-cells with progressive recruitment of more β-cells up to 12 mM glucose, when the vast majority of the cells are active.[34,35] Considering the glucose range where this heterogeneity becomes apparent, an overall shift towards greater glucose sensitivity in the *Pim3*$^{-/-}$ islets could account for both the increased basal insulin secretion relative to wildtype at 2 mM glucose, the increased insulin secretion at 8 mM and the lack of increased insulin secretion at 14 mM glucose. Although not directly assessed here, a putative role for Pim3 in setting the threshold for β-cell activation by glucose strongly resembles the reported role for Pim1 and Pim2 in the regulation of T-cell sensitivity to TCR/IL-2 activation.[19]

The elevated insulin secretion at 2 mM glucose observed in the isolated *Pim3*$^{-/-}$ islets was surprising considering the relative hypoinsulinemia found in *Pim3*$^{-/-}$ mice. Aside from a potential population shift in glucose sensitivity mentioned previously, the difference in basal insulin secretion could be secondary to extrinsic regulation of the β cell (e.g., alpha-adrenergic stimulation) in the whole animal that helps maintain euglycemia in a background of increased insulin sensitivity.[36] Indeed, the reduced serum insulin levels in the *Pim3*$^{-/-}$ mice at 0 and 30 minutes during a glucose tolerance test (**Fig. 3E**) suggest that *Pim3*$^{-/-}$ mice do extrinsically regulate insulin secretion in some capacity. In fact, the increased insulin sensitivity itself may be extrinsically regulated at the neuronal level as well. Recent studies demonstrate that insulin-sensitive neurons in the hypothalamus can rapidly regulate hepatic glucose production and potentiate the effect of circulating insulin on peripheral tissue through activation of the insulin signaling pathway in these neurons.[37,38] Considering Pim3 is significantly expressed in the CNS (and not well or consistently expressed in insulin-sensitive peripheral tissue),[17,19] the increased insulin sensitivity in *Pim3*$^{-/-}$ mice may be from alterations in insulin signaling in hypothalamic neurons. The underlying cause of this increased insulin sensitivity warrants further investigation.

The molecular mechanism underlying the secretion phenotype likely involves the regulation of ERK1/2 activity by Pim3. It was

recently shown that blocking ERK1/2 activation in MIN6 cells and isolated rat islets leads to reduced insulin secretion, specifically at earlier timepoints after glucose stimulation.[7] This effect is in line with our observations that augmented ERK1/2 activity after glucose stimulation temporally correlates with increased insulin secretion in isolated *Pim3*$^{-/-}$ islets. Furthermore, preliminary data where *Pim3*$^{-/-}$ islets were treated with the MEK inhibitor PD98059 suggest that directly inhibiting ERK1/2 activation appears to eliminate this augmented glucose-stimulated insulin secretion (**Suppl. Fig. 1**).

We show that Pim3 may regulate ERK1/2 activity through SOCS6. Pim3 physically interacts with SOCS6 and appears to regulate its stability. SOCS6 itself has been implicated in regulating ERK1/2 activity.[33,39] Our data suggest that SOCS6 would act as a negative regulator of insulin secretion, though *SOCS6*$^{-/-}$ mice show no changes in glucose or insulin tolerance.[32] *SOCS7*$^{-/-}$ mice do, however, exhibit enhanced insulin sensitivity and glucose tolerance.[40] The high degree of homology between SOCS6 and SOCS7 suggests the possibility of functional redundancy in the β-cell and potentially explains the absence of a phenotype in the *SOCS6*$^{-/-}$ mice. SOCS6 transgenic mice, despite reduced PI3 kinase activation in hepatocytes after in vivo insulin stimulation, paradoxically exhibited *improved* glucose and insulin tolerance.[31] None of these studies, however, examined the role of SOCS6 in the β-cell specifically so the full profile of SOCS6 function in glucose homeostasis remains unclear.

Aside from its role modulating ERK1/2 and SOCS6 activity, functional interactions between Pim3 and the pro-apoptotic protein BAD may further contribute to the regulation of β-cell function. Over-activation of the β-cell in response to glucose can potentially lead to excessive insulin secretion and undue metabolic stress leading to β-cell apoptosis. Through Pim3 phosphorylation of BAD at Ser^{112},[22] the anti-apoptotic pathway would be favored, thus promoting β-cell survival at the point of maximal glucose stimulation when Pim3 expression is greatest. Consistent with a role in regulating cell growth and survival, *Pim3*$^{-/-}$ islets are slightly, but significantly hypotrophic (**Fig. 3F**). The interaction between Pim3 and BAD may also relate to the insulin secretion phenotype observed in our study. Danial et al. show that phosphorylated BAD in the β-cell, particularly at Ser^{155}, stimulates insulin secretion by stimulating glucokinase activity on the mitochondrial membrane.[41] Though the role and regulation of serine phosphorylation in BAD is not fully understood, phosphorylation of Ser^{112} and/or Ser^{136} appears to regulate binding to 14-3-3 whereas phosphorylated Ser^{155} interacts with Bcl-X_L.[42,43] In *Pim3*$^{-/-}$ β-cells, there may be less BAD sequestered in the cytosol by 14-3-3 because of reduced Ser^{112} phosphorylation allowing more BAD to be available to interact with mitochondrial glucokinase and thus enhancing insulin secretion. Further studies are necessary to determine whether there is a direct connection between Pim3 activity and the role of BAD in insulin secretion, but this potential dual role of Pim3 in limiting insulin secretion is an exciting possibility.

In summary, we have identified Pim3 as a novel factor in the regulation of glucose-stimulated insulin secretion whereby Pim3 inhibits this process by limiting glucose-stimulated ERK1/2 activity through its effect on SOCS6. These data ascribe a new function to a member of a well-studied protein family and broadens our knowledge of signaling pathways responsible for regulating insulin secretion. Furthermore, the implication of Pim3 in generalized suppression of the activated β-cell further suggests that this kinase has a more global and central role in β-cell function. This may provide a novel therapeutic target for enhancing the β-cell response to glucose stimulation by improving insulin secretion and β-cell survival, and with potentially a combined effect on peripheral insulin sensitivity, may overcome the insulin resistance associated with type 2 diabetes.

Materials and Methods

Microarray analysis. Microarray analysis was performed as described previously.[24] Specifically, early-passage MIN6 murine pancreatic beta cells were grown in high-glucose DMEM (Invitrogen, Carlsbad, CA) supplemented with 10% heat-inactivated FBS (Invitrogen, Carlsbad, CA) and 28.4 μM 2-mercaptoethanol (Sigma-Aldrich, St. Louis, MO). Cells were then treated with 5.5 mM glucose DMEM, 10% FBS, 28.4 μM 2-mercaptoethanol for 24 hours and then stimulated with 25 mM glucose DMEM, 10% FBS, 28.4 μM 2-mercaptoethanol. Total RNA was prepared (Ambion, Austin, TX) at 0, 15, 30, 60, 180, 360 and 720 minutes after stimulation with 25 mM glucose and poly(A)$^+$ RNA was then isolated by using oligo-dT-conjugated latex beads (Qiagen, Valencia, CA). Double-stranded cDNA was then synthesized from 1 μg of poly(A)$^+$ RNA by using the Superscript Choice System (Invitrogen, Carlsbad, CA) with an oligo-dT primer containing a T7 RNA polymerase promoter (Genset, La Jolla, CA). Approximately 1.5 μl of the resulting cDNA was then used in an in vitro transcription reaction using Bioarray High Yield RNA Transcript Labeling Reagents (Enzo Diagnostics, Farmingdale, NY) and incorporating biotinylated CTP and UTP. In vitro transcription reactions yielded 50–70 μg biotin-labeled cRNA. Biotin-labeled cRNA was purified on a RNeasy affinity column (Qiagen, Valencia, CA) and fragmented at 94°C for 35 min in fragmentation buffer (40 mM Tris-acetate pH 8.1, 100 mM KOAc, 30 mM MgOAc). Hybridization solution (1 M NaCl, 20 mM EDTA, 100 mM 2-(*N*-morpholino) ethanesulfonic acid, 0.01% Tween 20) was used to prehybridize Affymetrix (Santa Clara, CA) Mu11K and Mu19K oligonucleotide microarrays for 30 min at 40°C. The prehybridization solution was removed and replaced with 200 μl of hybridization solution containing 0.05 μg/μl of fragmented cRNA. The arrays were hybridized for 16 h at 40°C. After hybridization, arrays were washed on an Affymetrix fluidics station and stained with streptavidin-phycoerythrin (hybridization solution, 2 mg/ml acetylated BSA and 5 μg/μl streptavidin R-phycoerythrin). (Molecular Probes, Invitrogen, Carlsbad, CA). After staining, arrays were washed extensively in fresh hybridization buffer. Arrays were scanned on a Hewlett-Packard GeneArray Scanner, and the data obtained were analyzed by using Affymetrix GENECHIP 3.2 software.

Immunofluorescence. Immunofluorescence was performed as described previously.[44] Briefly, pancreata were removed from mice,

fixed in formalin, and embedded in paraffin. Sections were then cut to a thickness of approximately 5 μm. Antigens were detected by affinity-purified rabbit polyclonal antibodies to Pim3 (1:50 dilution), guinea pig anti-glucagon (Millipore, Billerica, MA, 1:400 dilution), and mouse anti-insulin antibodies (Invitrogen, Carlsbad, CA, 1:500 dilution). Pim3 antibody was produced by immunizing rabbits with a synthetic peptide corresponding to residues 13–32 of mouse Pim3. Antibodies were purified by protein A and peptide-affinity chromatography. Fluorescently labeled secondary donkey antibodies (Jackson Immunoresearch, West Grove, PA, anti-rabbit, Cy5; anti-guinea pig Cy3; and anti-mouse, Cy2) at 1:200 dilution were used for detection. Fluorescence was then detected using the Olympus IX81 inverted fluorescent microscope (Olympus, Center Valley, PA) and images were analyzed using MetaMorph software (Universal Imaging, West Chester, PA).

Real-time PCR. Isolated islets were stimulated with glucose as described below, and islets were lysed in denaturation solution (Ambion, Austin, TX) to isolate RNA. Using the ToTALLY RNA isolation kit (Ambion, Austin, TX) RNA was isolated at each timepoint by phenol:choloform:IAA extraction and isopropanol precipitation. After determining total RNA concentration using A_{260}/A_{280} measurements made by spectrophotometer, cDNA was synthesized from approximately 1 μg of RNA using the iScript cDNA synthesis kit (Bio-Rad, Hercules, CA). The resulting cDNA was then used in the iQ SYBR Green supermix real-time PCR reaction (Bio-Rad, Hercules, CA). Reactions were set up as follows: 12.5 μL iQ SYBR Green Supermix (Bio-Rad, Hercules, CA), 10 pmol forward primer, 10 pmol reverse primer, 10 μL cDNA (1:100 dilution), and sterile water for a final volume of 25 μL. Standard curves at dilutions of 1:10, 1:100, and 1:1,000 were prepared for each primer set. Primers (Operon Qiagen, Valencia, CA) were designed to amplify each of the following two loci: *Pim3* (5'-AAG GAC ACG GTC TAC ACT GAC T-3' and 5'-ACA CCA TGT CGT AGA GCA GTA C-3') and *18S* (5'-GCT GGA ATT ACC GCG GCT-3' and 5'-CGG CTA CCA CAT CCA AGG AA-3'). PCR conditions were as follows: 95°C for 3 min (1X), [95°C for 10 s, 60°C for 30 s, 72°C for 30 s] (40x), 95°C for 1 min (1X), 55°C for 1 min (1X), 55°C for 10 s (80X). The setpoint temperature was increased after cycle 2 by 0.5°C. Melt curve analysis was performed in order to verify the amplification of a single PCR product. The threshold cycle (C_T) methodology was utilized to quantify relative amounts of mRNA and samples were corrected for discrepancies in the initial amount of RNA present by normalizing to the C_T of the 18S transcript, a transcript that is unchanged after glucose stimulation.

Generation of Pim3-deficient mice. *Pim3*$^{-/-}$ mice have been previously generated.[19] Mice were maintained on an FVB/N background and the care of all animals in these studies was in accordance with the National Institutes of Health and University of Chicago institutional guidelines.

Metabolic studies. Studies utilized male mice between 10 to 16 weeks of age. Insulin and glucose tolerance tests were performed as previously described.[45] Serum insulin levels were determined by performing the glucose tolerance test as before on anesthetized animals (inhaled Metofane dosed to effect) and obtaining blood at appropriate timepoints via retro-orbital bleed.[45] Insulin levels were determined using a sensitive rat insulin RIA kit (Millipore, Billerica, MA).

Islet isolation. Islets were isolated using an intraductal collagenase technique as described previously and were handpicked.[46] Briefly, islet isolation buffer (1X Hanks' Balanced Salt Solution, 10 mM HEPES, 1 mM $MgCl_2$, 1 mM $CaCl_2$, 5 mM glucose, 100 units/mL penicillin and 100 μg/mL streptomycin, pH 7.4) containing 0.375 mg collagenase P (Roche, Indianapolis, IN) per mL was infused into the pancreas via intraductal injection. After collagenase digestion of the pancreas, islets were washed twice with islet isolation buffer, and then handpicked using a Zeiss Stemi 2000-C stereo zoom microscope. Islets were then placed in 11.5 mM glucose RPMI 1640 (Invitrogen, Carlsbad, CA) supplemented with 10% heat-inactivated fetal bovine serum (Invitrogen, Carlsbad, CA), 100 units/mL penicillin and 100 μg/mL streptomycin (Invitrogen, Carlsbad, CA) and allowed to recover overnight at 37°C and 5% CO_2.

Islet perifusion. Perifusion experiments were performed as described previously using bicarbonate-buffered Krebs Ringer Buffer (KRB)[47] supplemented with BSA (0.2 g/L) with some modification. Specifically, each sample contained 45–50 islets, flow rate was 0.5 mL/min and fractions were collected every 2 minutes in a temperature-controlled multichamber perifusion system (ACUSYST-S, Cellex Biosciences, Minneapolis, MN). At the conclusion of the perifusion experiment, islets were lysed in PBS + 1% Triton X-100 to determine total insulin levels. Insulin concentration in eluted fractions and for total pancreatic insulin was determined by a double-antibody RIA using a rat insulin standard.[48]

Islets stimulation and total pancreatic insulin determination. Islets (40–45 per timepoint) were first incubated in 2.8 mM glucose RPMI 1640 with 100 units/mL penicillin and 100 μg/mL streptomycin for 3 hours at 37°C and 5% CO_2. With the exception of the islets used for T_0, islets were then stimulated with 16.7 mM glucose RPMI 1640 with 100 units/mL penicillin and 100 μg/mL streptomycin for 5, 10 and 30 minutes. Islets were then lysed in 2X Laemmli Buffer (Bio-Rad, Hercules, CA) and protein levels were determined using the RC DC protein assay (Bio-Rad, Hercules, CA). FBS was excluded from the quiescence media and stimulation media for optimal quiescence and to limit the extent of non-glucose stimulation in subsequent analysis. Lysates were then resolved by SDS-PAGE by loading equal protein mass and relative protein levels determined by western blot. Total pancreatic insulin was determined by ethanol-acid extraction as described previously.[49] Insulin concentrations were measured as described above.[48]

β-cell and acinar-cell size determination. Immuno-fluorescence and antigen labeling for beta cells were performed as described above. Nuclei were labeled by staining with 4',6-diamidino-2-phenylindole (DAPI) at a 1:1,000 dilution (Sigma-Aldrich, St. Louis, MO). Beta cell area in each section was defined by MetaMorph Software (Universal Imaging, West Chester, PA) and nuclei were counted manually on two separate occasions. Average beta cell size was determined by dividing the area of the region by the number of nuclei counted. Average acinar cell size was determined as with the insulin-positive region except regions, though similar in size to the islets, were arbitrarily drawn.

Cell culture. Early passage MIN6 cells (passages 18–29) were grown as described above and previously.[24] Low glucose media contained 0.5 mM glucose DMEM in the absence of fetal bovine serum (FBS) for optimal quiescence of MIN6 cells. Stimulation of cells was then performed in the absence of FBS or sodium pyruvate to minimize beta cell stimulation from non-glucose stimuli.

Adenovirus construction and infection. *Pim3* cDNA was cloned from MIN6 mRNA. Plasmid DNA encoding the kinase-dead Pim3 ($Pim3^{K68R}$) was constructed (QuikChange site-directed mutagenesis kit—Stratagene, La Jolla, CA) and a 5'-HA tag was added. The KD-Pim3 and KD-HA-Pim3-encoding fragments were then used to construct recombinant adenovirus using the Adeno-X Expression Systems 2 (Clontech, Mountain View, CA). HEK293 cells were maintained and viral titers were determined as in.[50]

MIN6 cells were infected with adenovirus at a multiplicity of infection of 2 for insulin secretion studies and 50 for crosslinking studies. Infection was performed in high glucose MIN6 media for 4 hours at 37°C in 5% CO_2. Cells were then rested in normal high glucose media at 37°C in 5% CO_2 for an additional 11 hours.

Construction and stimulation of MIN6 stable transfectants. MIN6 stable transfectants expressing SOCS6 cDNA (GenBank ID: BC085245) from the pcDNA 3.1/Zeo (-) expression vector (Invitrogen, Carlsbad, CA) were generated by electroporation and selection with Zeocin (Invitrogen, Carlsbad, CA). Expression of SOCS6 was detected by western blot (Fusion Antibodies, Belfast, northern Ireland). Cells were incubated in 0.5 mM glucose for 3 hours (T_0) and stimulated with 25 mM glucose for 5, 10 and 30 minutes.

MIN6 insulin secretion assay. MIN6 cells were plated in 24-well cell cultures plates to a confluence of 75–80% and infected with KD-Pim3- or β-galactosidase-expressing adenovirus (Clontech, Mountain View, CA) as described above. Cells were then incubated in low glucose (0.5 mM) MIN6 media for 3 hours at 37°C and 5% CO_2, the low glucose media was removed and cells were then stimulated with high glucose (25 mM) MIN6 stimulation media (650 μL) and incubated for an additional 60 minutes. Aliquots (150 μL) of media were removed 15, 30 and 60 minutes after glucose stimulation. Aliquots were spun for 2 minutes at 13,000 RPM and 100 μL was removed and used to determine insulin concentration. Insulin concentration was measured by a double-antibody RIA as described above.

GST fusion protein production and pulldown. Wt-Pim3- and KD-Pim3-GST fusion proteins were constructed using pGEX-4T-1 (Amersham Biosciences-GE Healthcare, Chalfont St. Giles, UK). Recombinant proteins were expressed and purified from BL21 *E. Coli* (Stratagene, La Jolla, CA).[51] Pulldown assays were performed as described[51] using 20 μg of Pim3-wt-GST, KD-Pim3-GST and GST proteins and MIN6 cell lysate from cells grown in 25 mM and 0.5 mM glucose.

Crosslinking and immunoprecipitation. MIN6 cells were infected with KD-HA-Pim3-expressing adenovirus, incubated in low glucose and stimulated with high glucose as described above. Cells were lysed before, 5, 10 and 30 minutes after stimulation in Buffer A[52] supplemented with 1.25 mM 3,3'-Dithiobis[sulfosuccinimidylpropionate] (DTSSP) (Pierce, Rockford, IL). Immunoprecipitations were performed on pre-cleared (with protein G-agarose) lysates by incubation with anti-HA antibody (1:200 dilution, Cell Signaling, Danvers, MA) and protein G-agarose (Roche, Indianapolis, IN) at 4°C with rotation. Proteins were eluted (and crosslinker cleaved) with 2X Laemmli buffer.

Statistical analysis. When applicable, results were presented as mean ± SEM. Unpaired Student's t-test was used to evaluate differences between results.

Acknowledgements

This work was supported by grants to GCW from the NIH (DK064042) and Takeda Pharmaceuticals (31879). This work was partly supported by the Medical Scientist National Research Service Award (T 32 GM07281) to G.V. and the Dutch Cancer Society (M.N.) to Dr. A. Berns. We would like to thank Dr. Louis Phillipson for helpful advice and for providing reagents and equipment and Dr. P. de Vos and Dr. R. van Amerongen for critical reading of the manuscript.

Note

Supplementary materials can be found at:
www.landesbioscience.com/supplement/VlacichISLETS2-5-sup.pdf

References

1. Docherty K, Steiner DF. Molecular and cellular biology of the Beta-cell. In: Portes DSR, ed. Ellenberg Rifkin's diabetes mellitus. Stamford, CT: Elsevier Science Publishing 1996; 29-48.
2. Meglasson MD, Matschinsky FM. Pancreatic islet glucose metabolism and regulation of insulin secretion. Diabetes Metab Rev 1986; 2:163-214.
3. Gembal M, Gilon P, Henquin JC. Evidence that glucose can control insulin release independently from its action on ATP-sensitive K^+ channels in mouse beta-cells. J Clin Invest 1992; 89:1288-95.
4. Taguchi N, Aizawa T, Sato Y, Ishihara F, Hashizume K. Mechanism of glucose-induced biphasic insulin release: K^+ channel-independent glucose action. Endocrinology 1995; 136:3942-8.
5. Kulkarni RN, Bruning JC, Winnay JN, Postic C, Magnuson MA, Kahn CR. Tissue-specific knockout of the insulin receptor in pancreatic beta cells creates an insulin secretory defect similar to that in type 2 diabetes. Cell 1999; 96:329-39.
6. MacDonald P, El-Kholy W, Riedel M, Salapatek A, Light P, Wheeler M. The multiple actions of GLP-1 on the process of glucose-stimulated insulin secretion. Diabetes 2002; 51:434-42.
7. Longuet C, Broca C, Costes S, Hani el H, Bataille D, Dalle S. Extracellularly regulated kinases 1/2 (p44/42 mitogen-activated protein kinases) phosphorylate synapsin I and regulate insulin secretion in the MIN6 beta-cell line and islets of Langerhans. Endocrinology 2005; 146:643-54.
8. Benes C, Poitout V, Marie JC, Martin-Perez J, Roisin MP, Fagard R. Mode of regulation of the extracellular signal-regulated kinases in the pancreatic ß-cell line MIN6 and their implication in the regulation of insulin gene transcription. Biochem J 1999; 340:219-25.
9. Frödin M, Sekine N, Roche E, Filloux C, Prentki M, Wolheim CB, et al. Glucose, other secretagogues and nerve growth factor stimulate mitogen-activated protein kinase in the insulin secreting β-cell line, INS-1. J Biol Chem 1995; 270:7882-9.
10. Khoo S, Cobb M. Activation of mitogen-activating protein kinase by glucose is not required for insulin secretion. Proc Natl Acad Sci USA 1997; 94:5599-604.
11. Taniguchi CM, Emanuelli B, Kahn CR. Critical nodes in signalling pathways: insights into insulin action. Nat Rev 2006; 7:85-96.
12. Khoo S, Griffen SC, Xia Y, Baer RJ, German MS, Cobb MH. Regulation of insulin gene transcription by ERK1 and ERK2 in pancreatic beta cells. J Biol Chem 2003; 278:32969-77.
13. Burns CJ, Howell SL, Jones PM, Persaud SJ. Glucose-stimulated insulin secretion from rat islets of Langerhans is independent of mitogen-activated protein kinase activation. Biochem Biophys Res Commun 1997; 239:447-50.

14. Allen J, Verhoeven E, Domen J, van der Valk M, Berns A. Pim-2 transgene induces lymphoid tumors, exhibiting potent synergy with c-myc. Oncogene 1997; 15:1133-41.
15. Dautry F, Weil D, Yu J, Dautry-Varsat A. Regulation of pim and myb mRNA accumulation by interleukin 2 and interleukin 3 in murine hematopoietic cell lines. J Biol Chem 1988; 263.
16. Cuypers HT, Selten G, Quint W, Zijlstra M, Maandag ER, Boelens W, et al. Murine leukemia virus-induced T-cell lymphomagenesis: integration of proviruses in a distinct chromosomal region. Cell 1984; 37:141-50.
17. Feldman JD, Vician L, Crispino M, Tocco G, Marcheselli VL, Bazan NG, et al. KID-1, a protein kinase induced by depolarization in brain. J Biol Chem 1998; 273:16535-43.
18. Fujii C, Nakamoto Y, Lu P, Tsuneyama K, Popivanova B, Kaneko S, et al. Aberrant expression of serine/threonine kinase Pim-3 in hepatocellular carcinoma development and its role in the proliferation of human hepatoma cell lines. Int J Cancer 2004; 114:209-18.
19. Mikkers H, Nawijn M, Allen J, Brouwers C, Verhoeven E, Jonkers J, et al. Mice deficient for all PIM kinases display reduced body size and impaired responses to hematopoietic growth factors. Mol Cell Biol 2004; 24:6104-15.
20. Peltola KJ, Paukku K, Aho TL, Ruuska M, Silvennoinen O, Koskinen PJ. Pim-1 kinase inhibits STAT5-dependent transcription via its interactions with SOCS1 and SOCS3. Blood 2004; 103:3744-50.
21. Chen XP, Losman JA, Cowan S, Donahue E, Fay S, Vuong BQ, et al. Pim serine/threonine kinases regulate the stability of Socs-1 protein. Proc Natl Acad Sci USA 2002; 99:2175-80.
22. Li YY, Popivanova BK, Nagai Y, Ishikura H, Fujii C, Mukaida N. Pim-3, a proto-oncogene with serine/threonine kinase activity, is aberrantly expressed in human pancreatic cancer and phosphorylates bad to block bad-mediated apoptosis in human pancreatic cancer cell lines. Cancer Res 2006; 66:6741-7.
23. Yan B, Zemskova M, Holder S, Chin V, Kraft A, Koskinen PJ, et al. The PIM-2 kinase phosphorylates BAD on serine 112 and reverses BAD-induced cell death. J Biol Chem 2003; 278:45358-67.
24. Webb GC, Akbar MS, Zhao C, Steiner DF. Expression profiling of pancreatic β cells: Glucose regulation of secretory and metabolic pathway genes. Proc Natl Acad Sci USA 2000; 97:5773-8.
25. Fox CJ, Hammerman PS, Cinalli RM, Master SR, Chodosh LA, Thompson CB. The serine/threonine kinase Pim-2 is a transcriptionally regulated apoptotic inhibitor. Genes Dev 2003; 17:1841-54.
26. Qian K, Wang L, Hickey E, Studts J, Barringer K, Peng C, et al. Structural basis of constitutive activity and a unique nucleotide binding mode of human Pim-1 kinase. J Biol Chem 2005; 280:6130-7.
27. van der Lugt NM, Domen J, Verhoeven E, Linders K, van der Gulden H, Allen J, et al. Proviral tagging in E mu-myc transgenic mice lacking the Pim-1 proto-oncogene leads to compensatory activation of Pim-2. EMBO J 1995; 14:2536-44.
28. Saris CJ, Domen J, Berns A. The pim-1 oncogene encodes two related protein-serine/threonine kinases by alternative initiation at AUG and CUG. EMBO J 1991; 10:655-64.
29. Bachmann M, Moroy T. The serine/threonine kinase Pim-1. Int J Biochem Cell Biol 2005; 37:726-30.
30. White M. Insulin signaling in health and disease. Science 2003; 302:1710-1.
31. Li L, Gronning LM, Anderson PO, Li S, Edvardsen K, Johnston J, et al. Insulin induces SOCS-6 expression and its binding to the p85 monomer of phosphoinositide 3-kinase, resulting in improvement in glucose metabolism. J Biol Chem 2004; 279:34107-14.
32. Krebs DL, Uren RT, Metcalf D, Rakar S, Zhang JG, Starr R, et al. SOCS-6 binds to insulin receptor substrate 4 and mice lacking the SOCS-6 gene exhibit mild growth retardation. Mol Cell Biol 2002; 22:4567-78.
33. Mooney RA, Senn J, Cameron S, Inamdar N, Boivin LM, Shang Y, et al. Suppressors of cytokine signaling-1 and -6 associate with and inhibit the insulin receptor. A potential mechanism for cytokine-mediated insulin resistance. J Biol Chem 2001; 276:25889-93.
34. Pipeleers D, Kiekens R, Ling Z, Wilikens A, Schuit F. Physiologic relevance of heterogeneity in the pancreatic beta-cell population. Diabetologia 1994; 37:57-64.
35. Kiekens R, In't Veld P, Mahler T, Schuit F, van de Winkle M, Pipeleers D. Differences in glucose recognition by individual rat pancreatic B cells are associated with intercellular differences in glucose-induced biosynthetic activity. J Clin Invest 1992; 89:117-25.
36. Lang P. Molecular mechanisms and regulation of insulin exocytosis as a paradigm of endocrine secretion. Eur J Biochem 1999; 259:3-17.
37. Obici S, Zhang BB, Karkanias G, Rossetti L. Hypothalamic insulin signaling is required for inhibition of glucose production. Nat Med 2002; 8:1376-82.
38. Ono H, Pocai A, Wang Y, Sakoda H, Asano T, Backer JM, et al. Activation of hypothalamic S6 kinase mediates diet-induced hepatic insulin resistance in rats. J Clin Invest 2008; 118:2959-68.
39. Bayle J, Letard S, Frank R, Dubreuil P, De Sepulveda P. Suppressor of cytokine signaling 6 associates with KIT and regulates KIT receptor signaling. J Biol Chem 2004; 279:12249-59.
40. Banks AS, Li J, McKeag L, Hribal ML, Kashiwada M, Accili D, et al. Deletion of SOCS7 leads to enhanced insulin action and enlarged islets of Langerhans. J Clin Invest 2005; 115:2462-71.
41. Danial NN, Walensky LD, Zhang CY, Choi CS, Fisher JK, Molina AJ, et al. Dual role of proapoptotic BAD in insulin secretion and beta cell survival. Nat Med 2008; 14:144-53.
42. Tan Y, Demeter MR, Ruan H, Comb MJ. BAD Ser-155 Phosphorylation Regulates BAD/Bcl-X_L Interaction and Cell Survival. J Biol Chem 2000; 275:25865-9.
43. Zha J, Harada H, Yang E, Jockel J, Korsmeyer SJ. Serine phosphorylation of death agonist BAD in response to survival factor results in binding to 14-3-3 not BCL-X_L. Cell 1996; 87:619-28.
44. Webb G, Akbar M, Zhao C, Steiner D. Continuous glucagon delivery via micro-osmotic pump suppresses multiple phenotypes in PC2 knockout mice. Diabetes 2002; 51:398-405.
45. Mauvais-Jarvis F, Ueki K, Fruman D, Hirshman M, Sakamoto K, Goodyear L, et al. Reduced expression of the murine p85alpha subunit of phosphoinositide 3-kinase improves insulin signaling and ameliorates diabetes. J Clin Invest 2002; 109:141-9.
46. Lacy PE, Kostianovsky M. Method for the isolation of intact islets of Langerhans from the rat pancreas. Diabetes 1967; 16:35-9.
47. Sturis J, Pugh W, Tang J, Ostrega D, Polonsky JS, Polonsky KS. Alterations in pulsatile insulin secretion in the Zucker diabetic fatty rat. Am J Physiol Endocrinol Metab 1994; 267:250-9.
48. Zhou YP, Pena JC, Roe MW, Mittal A, Levisetti M, Baldwin AC, et al. Overexpression of Bcl-x(L) in beta-cells prevents cell death but impairs mitochondrial signal for insulin secretion. Am J Physiol Endocrinol Metab 2000; 278:340-51.
49. Blondeau B, Lesage J, Czernichow P, Dupouy JP, Breant B. Glucocorticoids impair fetal Beta-cell development in rats. Am J Physiol Endocrinol Metab 2001; 281:592-9.
50. Greenberg C, Meredith K, Yan L, Brady M. Protein targeting to glycogen overexpression results in the specific enhancement of glycogen storage in 3T3-L1 adipocytes. J Biol Chem 2003; 278:30835-42.
51. Frangioni J, Neel B. Solubilization and purification of enzymatically active glutathione S-transferase (pGEX) fusion proteins. Anal Biochem 1993; 210:179-87.
52. Kim D, Sarbassov D, Ali S, King J, Latek R, Erdjument-Bromage H, et al. mTOR interacts with raptor to form a nutrient-sensitive complex that signals to the cell growth machinery. Cell 2002; 110:163-75.